

# C<sub>60</sub> Fullerene Nanoparticle Prevents $\beta$ -Amyloid Peptide Induced Cytotoxicity in Neuro 2A Cells

TAN-YI LU<sup>1#</sup>, PAI-FENG KAO<sup>1,2#</sup>, CHI-MING LEE<sup>3</sup>, SHENG-TUNG HUANG<sup>4</sup> AND CHUN-MAO LIN<sup>1\*</sup>

<sup>1</sup>. School of Medicine, Taipei Medical University, Taipei, Taiwan, R.O.C.

<sup>2</sup>. Division of Cardiology, Wan Fang Hospital, Taipei, Taiwan, R.O.C.

<sup>3</sup>. Core Facility Center, Taipei Medical University, Taipei, Taiwan, R.O.C.

<sup>4</sup>. Institute of Biotechnology, National Taipei University of Technology, Taipei, Taiwan, R.O.C.

(Received: December 9, 2010; Accepted: April 7, 2011)

## ABSTRACT

Oxidative stress, which is an early determinant of Alzheimer's disease (AD), is involved in mediating neuronal apoptosis in A $\beta$ -induced cell death. C<sub>60</sub> fullerenes are known to behave like a "radical sponge" as they can sponge up free radicals and act more effectively than other antioxidants. PEG-C<sub>60</sub>-3, a C<sub>60</sub> fullerene derivative, was investigated against  $\beta$ -amyloid (A $\beta$ )<sub>25-35</sub>-induced toxicity toward Neuro-2A cells in this study. PEG-C<sub>60</sub>-3 reduced A $\beta$ <sub>25-35</sub>-induced cytotoxicity, which showed an increasing cell viability with C<sub>60</sub> and A $\beta$ <sub>25-35</sub> co-treated cells. Moreover, the intracellular reactive oxygen species (ROS) accumulation caused by A $\beta$ -treated Neuro-2A cells was reduced by PEG-C<sub>60</sub>-3 co-treatment. Microarray for the analysis of gene expressions was investigated. Endoplasmic reticulum (ER) stress responsive genes, ion-channel, cell-cycle and anti-oxidant related cell responses were found to be associated with C<sub>60</sub> protective mechanism against A $\beta$ <sub>25-35</sub> treatment. The results offered new comprehension into the possible pathway of A $\beta$ <sub>25-35</sub> gene expression and C<sub>60</sub> protective mechanism. With the understanding of the roles of A $\beta$  and C<sub>60</sub> in cells, we can hopefully provide insight on therapeutic design using C<sub>60</sub> fullerene nanoparticles against A $\beta$ -associated diseases.

Key words: apoptosis, amyloid, fullerene, reactive oxygen species (ROS)

## INTRODUCTION

Amyloid plaques are protein deposits found abundantly in the brains of Alzheimer's patients. The plaques, along with neurofibrillary tangles, interfere with normal neuron functioning. Over the past decade, several hypotheses have been set forth to explain the pathophysiology of AD<sup>(1)</sup>. The mechanisms underlying AD and the events responsible for its progression remain unclear. It was confirmed that oxidative stress is involved in apoptotic mechanisms where production of excessive reactive oxidative species (ROS) can mediate neuronal apoptosis in A $\beta$ -induced cell death, resulting in senile plaque formation<sup>(2)</sup>. Once A $\beta$  peptide aggregates into amyloid fibrils with a cross  $\beta$ -sheet conformation, the fibril became neurotoxic partly due to the generation of its associated free radicals, followed by lipid peroxidation and protein oxidation as a result of oxidative stress<sup>(3)</sup>. Oxidant-induced oligomerization of A $\beta$  is recognized as an important factor in neuronal dysfunction and cellular apoptosis. Thus, antioxidants are used to prevent and cure associated diseases.

Water-soluble C<sub>60</sub> fullerene derivatives have been significantly studied due to the broad range of biological activities found for these compounds. It also has been shown to exhibit considerable *in vitro* biological activities, including cytotoxic, site-selective DNA cleavage and inhibition of HIV protease<sup>(4)</sup>. The exceptional radical-scavenging property of fullerene makes it a promising pharmacophore to target diseases caused by the overexpression of radicals<sup>(5,6)</sup>. When injected intravenously, it is distributed rapidly to various tissues and most of the material is retained in the body after one week. The fullerene molecules rapidly aggregate in water but disaggregate after entering the membrane interior. The compound was also able to penetrate the blood-brain barrier (BBB)<sup>(4,7)</sup>. The C<sub>60</sub> fulleropyrrolidine-thalidomide dyad (CLT) is an effective agent for suppressing the release of NO and TNF- $\alpha$  by the LPS-stimulated macrophages RAW264.7<sup>(8)</sup>. The fulleropyrrolidine-xanthine dyad can effectively suppress LPS-induced NO production<sup>(9)</sup>. These results suggest the possibility of using C<sub>60</sub> fullerene or fullerene dyad for treatment to support the pharmacological and non-pharmacological therapy of AD.

\* Author for correspondence. Tel: 886-2-27361661 ext. 3165;

Fax: 886-2-27387348; E-mail: cmlin@tmu.edu.tw

# These two authors contributed equally to this work.

## MATERIALS AND METHODS

### I. Chemicals and Reagents

3-(4,5-Dimethyl-2-thiazolyl)-2,5-diphenyl tetrazolium bromide (MTT) and dihydrorhodamine 123 (DHR123) were purchased from Sigma (St. Louis, MO, USA). All solvents used in this study were from Merck (Darmstadt, Germany). Dulbecco's modified Eagle's medium (DMEM), penicillin and streptomycin were obtained from Gibco BRL (Grand Island, NY, USA). The water-soluble C<sub>60</sub> fullerene (PEG-C<sub>60</sub>-3) was prepared according to a previously published study<sup>(8,9)</sup>. The structure is shown in Figure 1.

### II. Cell Culture

Mouse neuroblast Neuro-2A cells were grown in DMEM supplemented with 10% fetal bovine serum (Hyclone, Logan, UT, USA), 1.5 g/L sodium bicarbonate, 1% penicillin-streptomycin-amphotericin, 1% sodium pyrophosphate and 1% non-essential amino acids at 37°C in a humidified atmosphere with 5% CO<sub>2</sub> for 24 h before proceeding with the following experiments.

### III. Cell Viability Assay

The MTT assay to test the cytotoxicity of reagents and cell viability was carried out as described previously<sup>(10)</sup>. Cells (15,000 cells/well) were grown in supplemented culture medium. The cells were treated with Aβ<sub>25-35</sub> (0 - 15 μM) for 24 h, followed by the addition of MTT to the growing cultures at a final concentration of 0.5 mg/mL. The absorbance was measured with a spectrophotometer (Thermo Varioskan Flash, Vantaa, Finland) at 560 nm.

### IV. Intracellular Reactive Oxygen Species (ROS) Measurement

Levels of cellular oxidative stress were measured using the fluorescent probe, Dihydrorhodamine (DHR123), as described previously<sup>(11)</sup>. After treatment with these compounds for 12 h, the cells were incubated for 30 min in the presence of 20 μM of DHR123, followed by washing with phosphate-buffered saline (PBS). DHR123 is trapped mainly in the cytoplasm and is oxidized into highly fluorescent rhodamine 123 by intracellular ROS. The DCF fluorescence intensity of cells was measured using a confocal microscope (Leica TCS SP5, Bensheim, Germany).

### V. RNA Preparation and Complementary (c)DNA Chip Analysis

Total RNAs were extracted from Neuro-2A cells treated with or without 15 μM of Aβ<sub>25-35</sub> for 24 h using the TRI-reagent (Molecular Research Center, Cincinnati, OH, USA) following the manufacturer's instructions. Only RNA samples with an OD 260/280 ratio of 1.7 - 2.0 were used for

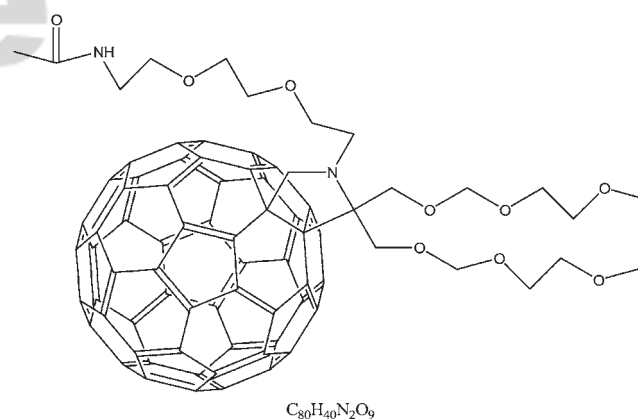


Figure 1. Structure of C<sub>60</sub> fullerene derivative, PEG-C<sub>60</sub>-3.

the microarray. The expression data from the cDNA microarrays were initially analyzed using BeadScan software (Illumina, San Diego, CA, USA). For the BeadArray analysis, the integrity of total RNA was assessed using the Agilent Bioanalyzer 2100 (Palo Alto, CA, USA), and RNA integrity (RIN) scores greater than 9.5 were present in all samples. RNA was amplified using the Illumina TotalPrep RNA amplification kit (Ambion, Applied Biosystems, Foster, CA, USA) with an *in vitro* transcription reaction period of 12 h. The quantity and quality of biotinylated, amplified cRNA were assessed using the Agilent Bioanalyzer 2100. Amplified cRNA at 1.5 μg per array was hybridized to Sentrix Mouse-6.v1 BeadChip arrays (Illumina) according to the manufacturer's directions. Hybridized BeadChip arrays were stained with Amersham fluorolink streptavidin-Cy3. BeadChip arrays were scanned with an Illumina BeadStation Scanner, and values with detection scores were compiled using BeadStudio Version 1.5.1.3 (Illumina) for data analysis. Only probe sets with at least a 1.5-fold change in gene expression compared to the controls were examined for the manual classification analysis using a gene ontology database (<http://www.godatabase.org/cgi-bin/amigo/go.cgi>) and published reports<sup>(12)</sup>.

### VI. Statistical Analysis

Unless otherwise indicated, results are represented as the mean ± SD of five replicates, and at least three separate experiments were performed. One-way analysis of variance (ANOVA) followed by Bonferroni's test was used to determine statistical significance for multiple comparisons, and Student's *t*-test was used between groups. A *p* value of less than 0.05 was accepted as statistically significant.

## RESULTS AND DISCUSSION

We evaluated the anti-cytotoxic effects of PEG-C<sub>60</sub>-3 on Aβ<sub>25-35</sub>-treated Neuro-2A cells. Treatment of Neuro-2A cells with Aβ<sub>25-35</sub> for 24 h decreased cell viability, as determined by an MTT assay (Figure 2). Neuro-2A cells treated with

Aβ<sub>25-35</sub> (15 μM) for 24 h in the absence of test compounds exhibited 60.7% viability; while viability of cells pretreated with PEG-C<sub>60</sub>-3 (5 - 15 μM) increased to 64.1%, 70.4% , and 86.0%, respectively. PEG-C<sub>60</sub>-3 displayed significant protection against Aβ cytotoxicity.

ROS formation visualized by confocal microscopy with the redox-sensitive fluorescent dye, DHR123 was shown in

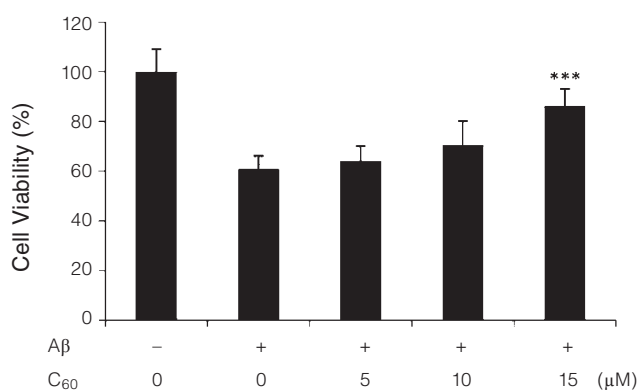


**Figure 2.** Cytoprotective effects of C<sub>60</sub> fullerene derivatives against β-amyloid (Aβ)<sub>25-35</sub>-induced toxicity of Neuro-2A cells. Cell viability of combined treatments with Aβ<sub>25-35</sub> (15 μM) and C<sub>60</sub> fullerene derivatives (0 - 15 μM) for 24 h. \*\*\* *p* < 0.001, versus Aβ treatment. The results are presented as the mean ± SD (n = 5). Cell viability was assessed by an MTT assay and one-way ANOVA followed by Bonferroni's test. The experiment is representative of more than three independent analyses with similar results.

Figure 3. Cells were located under bright-field optics and scanned once with a laser (excitation at 488 nm and emission at 510 nm). The fluorescence was more intense in Neuro-2A cells treated with Aβ<sub>25-35</sub> alone, which meant it contained more free radicals, compared to those treated with PEG-C<sub>60</sub>-3. The amount of ROS in Aβ-treated Neuro-2A cells was reduced by the addition of PEG-C<sub>60</sub>-3.

To further understand the gene expression profile upon Aβ and C<sub>60</sub> treatments in cells, a microarray experiment was performed. The data obtained were the representative of more than 3 independent experiments with similar results. Statistical tests and thresholds on fold changes were commonly used for the identification of altered gene expression by microarray assays. The scatter plots in Figure 4 indicated, graphically, the correlation between the platforms. BeadStudio Version 1.5.3.1 (Illumina) was used to analyze the expression data of cDNA. The plot on the left was the control versus PEG-C<sub>60</sub>-3 treatment, and the plot on the right showed the control versus Aβ-treatment. In general, there was reasonably good concordance between the platforms. One-point-five fold up- and down-regulated genes were shown in dots (Figure 4). Only genes with at least 1.5-fold changes were used to compare in the Venn diagrams (Figure 5). The Venn diagrams involved two sets: the left circle represented Aβ-treatment and the right circle represented PEG-C<sub>60</sub>-3 treatment of Neuro-2A cells. Figure 5A showed the number of down-regulated gene expression entities. There were 89 entities with Aβ-treatment and 162 entities

**Table 1.** Differentially expressed genes in Neuro 2A cells after Aβ and C<sub>60</sub> treatment

Gene name and function	Accession No.	Aβ <sup>a</sup>	Aβ + C <sub>60</sub>
Asparagine synthetase (ASNS)	NM_012055.1	0.64	0.78
Activating transcription factor 5 (ATF5); RNA polymerase II transcription factor activity	NM_030693.1	0.64	0.69
Voltage-dependent calcium channel gamma-3 subunit (CACNG3); voltage-gated ion channel activity	NM_019430.1	0.61	0.77
Cyclin-dependent kinase inhibitor 1A( CDKN1A); protein kinase inhibitor activity	NM_007669.2	0.64	0.80
Transcriptional repressor (CTCF); nucleic acid binding	NM_001081387.1	0.61	0.80
Insulin-like growth factor-binding protein 6 (IGFBP6); insulin-like growth factor binding	NM_008344.1	0.66	0.73
Lung carcinoma derived myc gene (LMYC1); transcription factor activity	NM_008506.2	0.63	0.76
Myeloid differentiation primary response (MYD116); cell differentiation	NM_008654.1	0.54	0.70
Neoplastic progression 3 (NPN3); antioxidative activity	NM_029688.2	0.63	0.75
Nuclear RNA export factor 7(NXF7); transferase activity	NM_130888.1	0.61	0.73
Oral-facial-digital syndrome 1 protein (OFD1); molecular_function	NM_177429.2	0.67	0.87
Insulin gene enhancer protein (ISL1); sequence-specific DNA binding	NM_021459.2	1.66	1.33
Paired mesoderm homeobox gene (PMX2B); transcription factor	AK052579	1.72	1.28
Ribosomal protein S28 (RPS28); ribonucleoprotein complex	NM_016844.1	1.56	0.77
Tissue inhibitor of metalloproteinases 2 (TIMP2); metalloproteinase inhibitor 2	NM_011594.2	1.64	1.39
Transient receptor potential cation channel, subfamily M, member 2 (TRPM2); hydrolase activity	NM_138301.1	1.52	1.18

<sup>a</sup>: up-regulated gene expression > 1.5-fold change (ratio > 1.5); down-regulated gene expression > 1.5-fold change (ratio < 0.66)

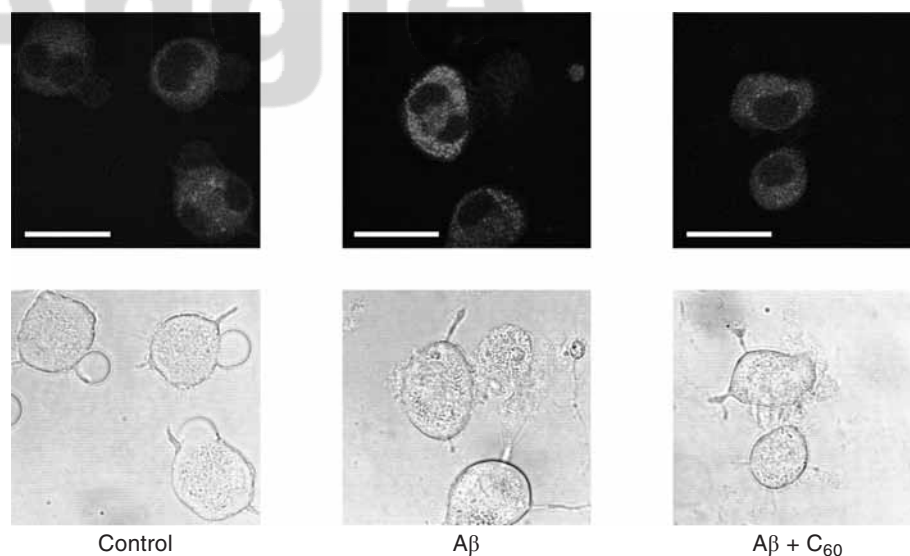


**Figure 3.** Effects of PEG-C<sub>60</sub>-3 on  $\beta$ -amyloid ( $A\beta$ )<sub>25-35</sub>-induced intracellular oxidative stress in Neuro-2A cells. DHR123 fluorescence imaged by laser confocal microscopy with treatments of vehicle control (0.1% DMSO) (left),  $A\beta$ <sub>25-35</sub> (15  $\mu$ M) alone (middle), and a combination of  $A\beta$ <sub>25-35</sub> and PEG-C<sub>60</sub>-3 (10  $\mu$ M) for 12 h (right). bar = 25  $\mu$ m.

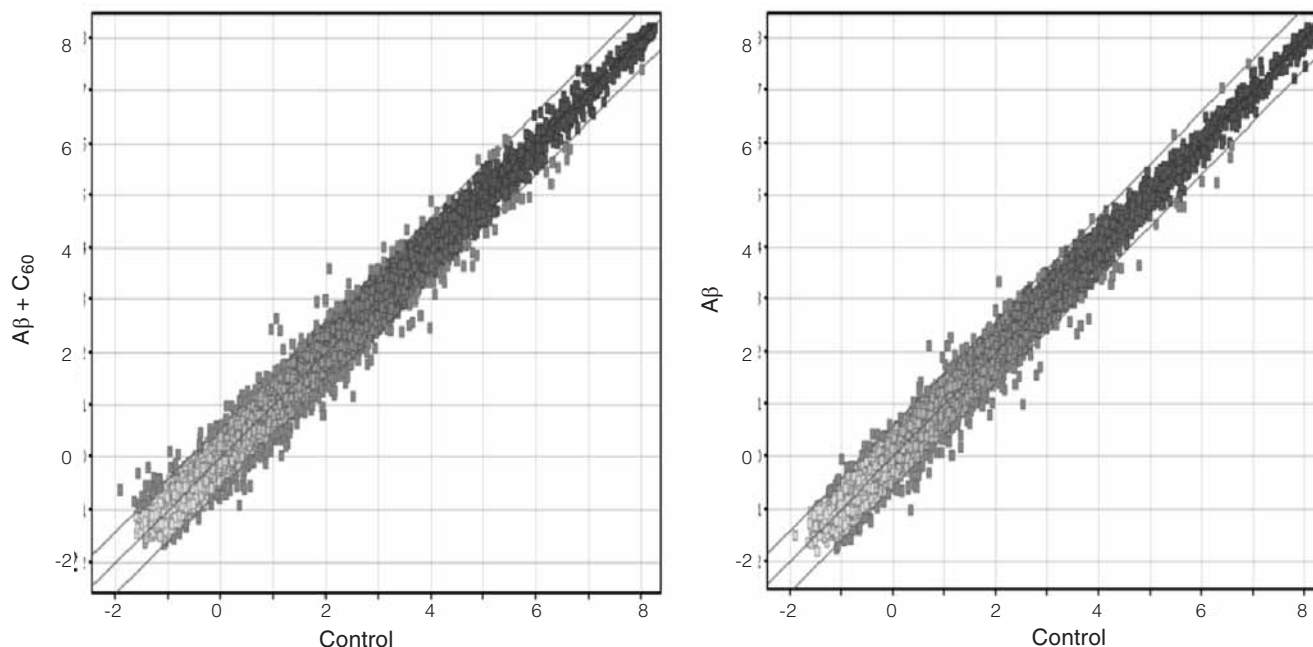


**Figure 4.** Scatter plot of 1.5 fold up- and down-regulated gene expression for microarray assay. Scatter plot analysis was determined by Bead-Studio Version 1.5.1.3 (Illumina). RNA samples with an OD 260/280 ratio of 1.7 - 2.0 were used for the microarray. The quantity and quality of biotinylated, amplified cRNA were assessed using the Agilent Bioanalyzer 2100.

with PEG-C<sub>60</sub>-3 treatment; nevertheless, they corresponded to points in the area where two circles overlapped, which were 57 down-regulated entities. The up-regulated gene expression was shown in Figure 5B. Fifty-one entities were treated with  $A\beta$ , whereas 105 entities were treated with PEG-C<sub>60</sub>-3. The overlapping area of the two circles comprised 16 entities, which were up-regulated with both treatments.

We observed the treatment of Neuro-2A cells with  $A\beta$ -induced alterations of several gene expressions. The

expressions of 32 down-regulated and 35 up-regulated gene entities were further correlated to their known biological functions using gene ontology databases. Table 1 showed the genes and their descriptions in  $A\beta$  and PEG-C<sub>60</sub>-3 treatment. These included genes coding for transcription factor, growth factor, ion-channel, transferase and cell differentiation activity.  $A\beta$  was known to induce intracellular oxidative stress by upregulating ROS production and causing mitochondrial membrane aberrations in nerve cells. The increased level of

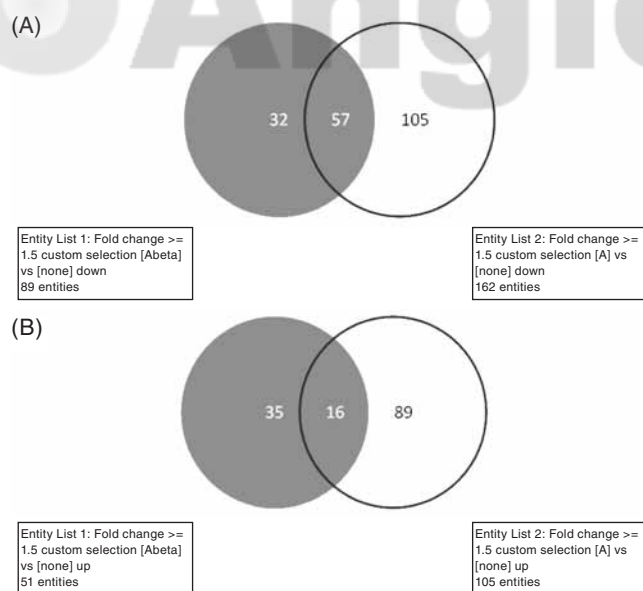


**Figure 5.** Venn diagram with the number of genes present in each platform and genes in common between platforms. (A) shows the number of down-regulated gene expression entities; (B) shows the number of up-regulated gene expression entities. BeadChip arrays were scanned with an Illumina BeadStation Scanner and values with detection scores were compiled using BeadStudio Version 1.5.1.3 (Illumina) for data analysis. Only probe sets with at least a 1.5-fold change in gene expression compared to the controls were examined for the manual classification analysis using a gene ontology database.

oxidative stress in the AD brain is reflected by the increased brain content of iron (Fe) and copper (Cu), both capable of stimulating free radical formation, increasing protein and DNA oxidation in the AD brain, enhancing lipid peroxidation, decreasing the level of cytochrome c oxidase and advanced glycation end products (AGEs), carbonyls, malondialdehyde (MDA), peroxynitrite and heme oxygenase-1 (HO-1). AGEs, mainly through their interaction with receptors for AGEs (RAGEs), further activate signaling pathways and induce the formation of pro-inflammatory cytokines, such as interleukin-6 (IL-6)<sup>(13)</sup>.

With A $\beta$  treatment, gene expressions with a ratio greater than 1.5 were up-regulated genes and those having a ratio smaller than 0.66 were down-regulated genes (Table 1). Transcription from the ASNS gene was increased in response to either amino acid (amino acid response) or glucose (ER stress response) deprivation<sup>(14)</sup>. Transcription factors ATF4 and ATF3 bound to the upstream region of the ASNS (asparagine synthetase) gene were functioned as mammalian ER-stress-responsive sequences<sup>(15)</sup>. ATF5 ER stress-related genes are bZIP transcription factors that forms homodimers, which, at least *in vitro*, bind to the cAMP response element (CRE). In addition, ATF5 represses cAMP-induced transcription in intact cells<sup>(16,17)</sup> and has been shown to inhibit apoptosis<sup>(18)</sup>. Available evidence suggests that genes encoding brain expressed voltage-gated calcium channels, including CACNG3 on chromosome, may represent susceptibility loci for CAE (childhood absence epilepsy)<sup>(19)</sup> and neuron

cells in this study. Cyclin-dependent kinase inhibitor 1A (CDKN1A) is implicated in the regulation of cell growth and cell response to DNA damage<sup>(20)</sup>. It also plays a role in the protection of cells against apoptosis and its expression is essential to maintain cell survival during differentiation of several cell lineages<sup>(21)</sup>. The CTCF-like protein, CTCFL, is a DNA-binding factor that regulates the transcriptional program of mammalian male germ cells<sup>(22)</sup>. It is also pivotal for the up-regulation of APP (amyloid precursor protein) expression during synaptogenesis in primary neurons<sup>(23)</sup>.

Over-expression of IGFBP-6 significantly suppresses the proliferation, invasion and metastatic activity of NPC (nasopharyngeal carcinoma) cells and increases their apoptosis<sup>(24)</sup>. Lmyc 1 gene encodes for a transcription factor that is believed to regulate expression of 15% of all genes<sup>(25)</sup>. This means that in addition to its role as a classical transcription factor, Myc also regulates global chromatin structure by regulating histone acetylation both in gene-rich regions and at sites far from any known gene<sup>(26)</sup>. MYD116 (also known as gadd34) is the murine homologue of growth arrest- and DNA damage-inducible genes, a gene family implicates in growth arrest and apoptosis induced by endoplasmic reticulum dysfunction<sup>(27)</sup>; hence, it was reported to influence cell survival<sup>(28)</sup>. Peroxiredoxins (Prx) are neuroprotective enzymes that protect neurons against oxidative stress. However, they can be inactivated through hyperoxidation of their active site cysteine, taking place in the brain in response to oxidative insults, such as stroke and aging. Sulfiredoxin (Srxn1), also known as neoplastic progression protein 3 (Npn3), is an inducible gene whose expression promoted the reduction of hyperoxidized Prx and protection against peroxide-induced death<sup>(29)</sup>. NPN3 (SRXN1) enzyme is involved in antioxidant metabolism by re-activating peroxiredoxins, which are a group of peroxidases, when these enzymes are inhibited by over-oxidation<sup>(30)</sup>. It is upregulated by an exceptionally large fold-magnitude in microarray studies of oxidative stress<sup>(31)</sup>. Nuclear RNA export factor 7 (NXF7) associates with translating ribosomes, stress granules (SGs) and processing bodies (P-bodies), the latter two of which are believed to be cytoplasmic sites of storage, degradation and/or sorting of mRNAs<sup>(32)</sup>. OFD1, a prolyl 4-hydroxylase-like 2-oxoglutarate dioxygenase, controls the oxygen-dependent stability of Sre1N. In the presence of oxygen, OFD1 accelerates the degradation of Sre1N, but under low oxygen, it is inhibited and Sre1N accumulates. Sre1, the fission yeast sterol regulatory element-binding protein, is an ER membrane-bound transcription factor that controls adaptation to low oxygen growth<sup>(33)</sup>. Oral-facial-digital syndrome type I (OFD1 mutation) is associated with the dysfunction of primary cilia, a microtubule-based cellular projection that mediates multiple signaling pathways. Centrioles represent the principal microtubule organizing centers of animal cells and Ofd1 acts at the distal centriole to stabilize centriolar microtubules at a defined structure and length and reveals the importance of centriole length control in centrosome function<sup>(34)</sup>. The above mentioned genes exhibited greater than 1.5-fold changes with down-regulated expression. PEG-C<sub>60</sub>-3 co-treatment reversed the changes in gene expression.

Transcription factor, Islet1 (ISL1) is a neuronal differentiation marker<sup>(35)</sup> that was reported to be associated with motor-axon differentiation<sup>(36)</sup>. PMX2B is also a transcription factor that plays an important role in the development of oculomotor nerves and regulates the expression of both tyrosine hydroxylase and dopamine beta-hydroxylase genes<sup>(37)</sup>. Ribosomal protein S28 (RPS28) gene encodes a ribosomal protein that is a component of the 40S sub-unit. The protein belongs to the S28E family of ribosomal proteins. The 5' leader regions of RPS28 mRNAs are found to harbour 8-11 pyrimidine tracts, which suggest similarities to regulatory stretches that control the translation of mRNAs for ribosomal proteins in animals<sup>(38)</sup>. R-protein depletion, with a few exceptions, leads to the accumulation of specific rRNA precursors, highlighting their individual roles in rRNA processing<sup>(39)</sup>. A stress, virus infection, triggers tissue inhibitor of matrix metalloproteinase 2 (TIMP2) upregulation in hepatic cells<sup>(40)</sup>, and the upregulated TIMP2 is reported to be associated with the neuroprotection against hyperoxic damage<sup>(41)</sup>. TIMP2 seemed to be elicited upon amyloid-beta treatment in Neuro-2A cells (1.64 fold), while PEG-C<sub>60</sub>-3 co-treatment reduced the stress-induced protective mechanism. TRPM2, a type of Nudix hydrolase, is a plasma membrane channel for Ca<sup>2+</sup> and Na<sup>+</sup> flowing into the neuronal cell. It is activated by oxidative stress, mediated cell death and inflammation, and was reported to be related to H<sub>2</sub>O<sub>2</sub> and amyloid  $\beta$ -peptide induced striatal cell death<sup>(42)</sup>. In this study, PEG-C<sub>60</sub>-3 and A $\beta$  co-treatment could reverse amyloid  $\beta$ -peptide induced TRPM2-upregulation. A $\beta$ -treated cells trigger the signaling cell cycle stimulating repair and protect cells to avoid cell apoptosis through the changes of gene expression. The above mentioned genes exhibited greater than 1.5-fold changes with up-regulated expression with A $\beta$  treatment. C<sub>60</sub> co-treatment reversed the changes in gene expression. These results suggested that C<sub>60</sub> showed a reverse effect on A $\beta$ -treated Neuro-2A cells.

In summary, we used oligonucleotide microarrays to identify and profile the expression of genes in Neuro-2A cells upon A $\beta$  and PEG-C<sub>60</sub>-3 co-treatment. In response to A $\beta$  exposure for 24 h, 16 up-regulated and down-regulated genes were elucidated to correlate the cytoprotective effect of PEG-C<sub>60</sub>-3 that might result from intracellular oxidative stress alleviation, ion-channel and transporter homeostasis, cell cycle regulation, and modulation in transcription factor activity thus protected from cell apoptosis.

#### ACKNOWLEDGMENTS

This study was supported by the grants from the Center of Excellence for Clinical Trial and Research in Neuroscience (DOH99-TD-B-111-003) and Taipei Medical University-Wan Fang Hospital (98TMU-WFH-03-2).

#### REFERENCES

- Hardy, J., Chartier-Harlin, M. C., and Mullan, M. 1992. Alzheimer disease: the new agenda. *Am. J. Hum. Genet.* 50: 648-651.
- Zheng, L., Marcusson, J., and Terman, A. 2006. Oxidative stress and Alzheimer disease: the autophagy connection? *Autophagy* 2: 143-145.
- Butterfield, D. A. and Lauderback, C. M. 2002. Lipid peroxidation and protein oxidation in Alzheimer's disease brain: potential causes and consequences involving amyloid beta-peptide-associated free radical oxidative stress. *Free Radic. Biol. Med.* 32: 1050-1060.
- Yamago, S., Tokuyama, H., Nakamura, E., Kikuchi, K., Kananishi, S., Sueki, K., Nakahara, H., Enomoto, S. and Ambe, F. 1995. In vivo biological behavior of a water-miscible fullerene: <sup>14</sup>C labeling, absorption, distribution, excretion and acute toxicity. *Chem. Biol.* 2: 385-389.
- Sitharaman, B., Zakharian, T. Y., Saraf, A., Misra, P., Ashcroft, J., Pan, S., Pham, Q. P., Mikos, A. G., Wilson, L. J. and Engler, D. A. 2008. Water-soluble fullerene (C<sub>60</sub>) derivatives as nonviral gene-delivery vectors. *Mol. Pharm.* 5: 567-578.
- Dugan, L. L., Turetsky, D. M., Du, C., Lobner, D., Wheeler, M., Almlie, C. R., Shen, C. K., Luh, T. Y., Choi, D. W. and Lin, T. S. 1997. Carboxyfullerenes as neuroprotective agents. *Proc. Natl. Acad. Sci. U.S.A.* 94: 9434-9439.
- Wong-Ekkabut, J., Baoukina, S., Triampo, W., Tang, I. M., Tieleman, D. P. and Monticelli, L. 2008. Computer simulation study of fullerene translocation through lipid membranes. *Nat. Nanotechnol.* 3: 363-368.
- Huang, S. T., Ho, C. S., Lin C. M., Fang H. W. and Peng, Y. X. 2008. Development and biological evaluation of C(60) fulleropyrrolidine-thalidomide dyad as a new anti-inflammation agent. *Bioorg. Med. Chem.* 16: 8619-8626.
- Huang, S. T., Liao, J. S., Fang, H. W. and Lin, C. M. 2008. Synthesis and anti-inflammation evaluation of new C60 fulleropyrrolidines bearing biologically active xanthine. *Bioorg. Med. Chem. Lett.* 18: 99-103.
- Lin, H. C., Tsai, S. H., Chen, C. S., Chang, Y. C., Lee, C. M., Lai, Z. Y. and Lin, C. M. 2008. Structure-activity relationship of coumarin derivatives on xanthine oxidase-inhibiting and free radical-scavenging activities. *Biochem. Pharmacol.* 75: 1416-1425.
- Keller, J. N., Guo, Q., Holtsberg, F. W., Bruce-Keller, A. J. and Mattson, M. P. 1998. Increased sensitivity to mitochondrial toxin-induced apoptosis in neural cells expressing mutant presenilin-1 is linked to perturbed calcium homeostasis and enhanced oxyradical production. *J. Neurosci.* 18: 4439-4450.
- Harman, A. N., Kraus, M., Bye, C. R., Byth, K., Turville, S. G., Tang, O., Mercier, S. K., Nasr, N., Stem, J. L., Slobodman, B., Driessen, C. and Cunningham, A. L. 2009. HIV-1-infected dendritic cells show 2 phases of gene expression changes, with lysosomal enzyme activity decreased during the second phase. *Blood* 114: 85-94.
- Jomova, K., Vondrakova, D., Lawson, M. and Valko, M. 2010. Metals, oxidative stress and neurodegenerative

- disorders. *Mol. Cell Biochem.* 345: 91-104.
14. Pan, Y., Chen, H., Siu, F. and Kilberg, M. S. 2003. Amino acid deprivation and endoplasmic reticulum stress induce expression of multiple activating transcription factor-3 mRNA species that, when overexpressed in HepG2 cells, modulate transcription by the human asparagine synthetase promoter. *J. Biol. Chem.* 278: 38402-38412.
  15. Gjymishka, A., Su, N. and Kilberg, M. S. 2009. Transcriptional induction of the human asparagine synthetase gene during the unfolded protein response does not require the ATF6 and IRE1/XBP1 arms of the pathway. *Biochem. J.* 417: 695-703.
  16. Pati, D., Meistrich, M. L. and Plon, S. E. 1999. Human Cdc34 and Rad6B ubiquitin-conjugating enzymes target repressors of cyclic AMP-induced transcription for proteolysis. *Mol. Cell Biol.* 19: 5001-5013.
  17. Peters, C. S., Liang, X., Li, S., Kannan, S., Peng, Y., Taub, R. and Diamond, R. H. 2001. ATF-7, a novel bZIP protein, interacts with the PRL-1 protein-tyrosine phosphatase. *J. Biol. Chem.* 276: 13718-13726.
  18. Persengiev, S. P., Devireddy, L. R. and Green, M. R. 2002. Inhibition of apoptosis by ATFx: a novel role for a member of the ATF/CREB family of mammalian bZIP transcription factors. *Genes Dev.* 16: 1806-1814.
  19. Everett, K. V., Chioza, B., Aicardi, J., Aschauer, H., Brouwer, O., Callenbach, P., Covanis, A., Dulac, O., Eeg-Olofsson, O., Feucht, M., Friis, M., Goutieres, F., Guerrini, R., Heils, A., Kjeldsen, M., Lehesjoki, A. E., Makoff, A., Nabbout, R., Olsson, I., Sander, T., Siren, A., McKeigue, P., Robinson, R., Taske, N., Rees, M. and Gardiner, M. 2007. Linkage and association analysis of CACNG3 in childhood absence epilepsy. *Eur. J. Hum. Genet.* 15: 463-472.
  20. Harper, J. W., Adami, G. R., Wei, N., Keyomarsi, K. and Elledge, S. J. 1993. The p21 Cdk-interacting protein Cip1 is a potent inhibitor of G1 cyclin-dependent kinases. *Cell* 75: 805-816.
  21. Asada, M., Yamada, T., Ichijo, H., Delia, D., Miyazono, K., Fukumuro, K. and Mizutani, S. 1999. Apoptosis inhibitory activity of cytoplasmic p21(Cip1/WAF1) in monocytic differentiation. *EMBO J.* 18: 1223-1234.
  22. Campbell, A. E., Martinez, S. R. and Miranda, J. J. L. 2010. Molecular architecture of CTCFL. *Biochemical and Biophysical Research Communications* 396: 648-650.
  23. Yang, Y., Quitschke, W. W., Vostrov, A. A. and Brewer, G. J. 1999. CTCF is essential for up-regulating expression from the amyloid precursor protein promoter during differentiation of primary hippocampal neurons. *J. Neurochem.* 73: 2286-2298.
  24. Kuo, Y. S., Tang, Y. B., Lu, T. Y., Wu, H. C. and Lin, C. T. 2010. IGFBP-6 plays a role as an oncosuppressor gene in NPC pathogenesis through regulating EGR-1 expression. *J. Pathol.* 222: 299-309.
  25. Gearhart, J., Pashos, E. E. and Prasad, M. K. 2007. Pluripotency Redux -- advances in stem-cell research. *N. Engl. J. Med.* 357: 1469-1472.
  26. Cotterman, R., Jin, V. X., Krig, S. R., Lemen, J. M., Wey, A., Farnham, P. J. and Knoepfler, P. S. 2008. N-Myc regulates a widespread euchromatic program in the human genome partially independent of its role as a classical transcription factor. *Cancer Res.* 68: 9654-9662.
  27. Doutheil J., Althausen, S., Gissel, C. and Paschen, W. 1998. Activation of MYD116 (gadd34) expression following transient forebrain ischemia of rat: implications for a role of disturbances of endoplasmic reticulum calcium homeostasis. *Glueterstr.* 50: 50931.
  28. White, F., McCaig, D., Brown, S. M., Graham, D. I., Harland, J. and Macrae, I. M. 2004. Up-regulation of a growth arrest and DNA damage protein (GADD34) in the ischaemic human brain: implications for protein synthesis regulation and DNA repair. *Neuropathol. Appl. Neurobiol.* 30:683-691.
  29. Soriano, F. X., Papadia, S., Bell, K. F. and Hardingham, G. E. 2009. Role of histone acetylation in the activity-dependent regulation of sulfiredoxin and sestrin 2. *Epigenetics.* 4: 152-158.
  30. Jönsson, T. J., Lowther, W. T. 2007. The peroxiredoxin repair proteins. *Subcell. Biochem.* 44: 115-141.
  31. Findlay, V. J., Townsend, D. M., Morris, T. E., Fraser, J. P., He, L. and Tew, K. D. 2006. A novel role for human sulfiredoxin in the reversal of glutathionylation. *Cancer Res.* 66: 6800-6806.
  32. Katahira, J., Miki, T., Takano, K., Maruhashi, M., Uchikawa, M., Tachibana, T. and Yoneda, Y. 2008. Nuclear RNA export factor 7 is localized in processing bodies and neuronal RNA granules through interactions with shuttling hnRNPs. *Nucleic Acids Res.* 36: 616-628.
  33. Lee, C. Y., Stewart, E. V., Hughes, B. T. and Espenshade, P. J. 2009. Oxygen-dependent binding of Nro1 to the prolyl hydroxylase Ofd1 regulates SREBP degradation in yeast. *EMBO J.* 28: 135-143.
  34. Singla, V., Romaguera-Ros, M., Garcia-Verdugo, J. M. and Reiter, J. F. 2010. Ofd1, a human disease gene, regulates the length and distal structure of centrioles. *Dev. Cell.* 18: 410-424.
  35. Pfaff, S. L., Mendelsohn, M., Stewart, C. L., Edlund, T. and Jessell, T. M. 1996. Requirement for LIM homeobox gene Isl1 in motor neuron generation reveals a motor neuron-dependent step in interneuron differentiation. *Cell* 84: 309-320.
  36. Avraham, O., Hadas, Y., Vald, L., Hong, S., Song, M. R. and Klar, A. 2010. Motor and dorsal root ganglion axons serve as choice points for the ipsilateral turning of dI3 axons. *J. Neurosci.* 30: 15546-15557.
  37. Ide, M., Yamada, K., Toyota, T., Iwayama, Y., Ishitsuka, Y., Minabe, Y., Nakamura, K., Hattori, N., Asada, T., Mizuno, Y., Mori, N. and Yoshikawa, T. 2005. Genetic association analyses of PHOX2B and ASCL1 in neuropsychiatric disorders: evidence for association of ASCL1 with Parkinson's disease. *Hum. Genet.* 117: 520-527.
  38. Giannino, D., Frugis, G., Ticconi, C., Florio, S., Mele, G., Santini, L., Cozza, R., Bitonti, M. B., Innocenti, A. and Mariotti, D. 2000. Isolation and molecular

- characterisation of the gene encoding the cytoplasmic ribosomal protein S28 in *Prunus persica* [L.] Batsch. *Mol. Gen. Genet.* 263: 201-212.
39. Robledo, S., Idol, R. A., Crimmins, D. L., Ladenson, J. H., Mason, P. J. and Bessler, M. 2008. The role of human ribosomal proteins in the maturation of rRNA and ribosome production. *RNA.* 14: 1918-1929.
40. Gieseler, R. K., Marquitan, G., Schlattjan, M., Sowa, J. P., Bechmann, L. P., Timm, J., Roggendorf, M., Gerken, G., Friedman, S. L. and Canbay, A. 2010. Hepatocyte apoptotic bodies encasing nonstructural HCV proteins amplify hepatic stellate cell activation: implications for chronic hepatitis C. *J. Viral. Hepat.* (In press)
41. Zhu, Y., Valter, K. and Stone, J. 2010. Environmental damage to the retina and preconditioning: contrasting effects of light and hyperoxic stress. *Invest Ophthalmol. Vis. Sci.* 51: 4821-4830.
42. Nazıroğlu M. 2010. TRPM2 Cation Channels, Oxidative Stress and Neurological Diseases: Where Are We Now? *Neurochem. Neurochem. Res.* 36: 355-366.